*Desalination and Water Treatment*
www.deswater.com

doi: 10.5004/dwt.2019.23266

138 (2019) 368–378
January

# Adsorption of light green anionic dye from solution using polyethyleneimine-modified carbon nanotubes in batch mode

Yifan Gu, Mingyu Liu, Mengmeng Yang, Weili Wang, Shusheng Zhang, Runping Han*

*College of Chemistry and Molecular Engineering, Zhengzhou University, 100 Kexue Road, Zhengzhou 450001 China, Tel. +86 371 67781757; Fax: +86 371 67781556; emails: rphan67@zzu.edu.cn (R. Han), 503153641@qq.com (Y. Gu), lmylittlerain@163.com (M. Liu), 1582415059@qq.com (M. Yang), 1063455250@qq.com (W. Wang), zsszz@126.com (S. Zhang)*

Received 5 July 2018; Accepted 9 October 2018

**ABSTRACT**

Polyethyleneimine (PEI)-functionalized carboxylated multi-walled carbon nanotubes (MWCNTs) were used as an adsorbent (PEI-CNTs) to adsorb light green (LG) dyes (anionic dye) from solution. The structure and morphology of PEI-CNTs was characterized by transmission electron microscope, Fourier-transform infrared (FTIR) spectroscopy, Raman spectroscopy, and X-ray photoelectron spectroscopy (XPS). FTIR and XPS results showed that PEI was successfully loaded on MWCNTs. Raman analysis showed that the basic structure of MWCNTs did not change after the modification of PEI. The effects of pH and coexisting ions on the adsorption properties were studied. Batch adsorption and kinetic studies showed that the PEI-CNTs nanocomposite materials were efficient to remove LG from solution. The optimum condition for adsorption was pH 3. The adsorption of LG solution reached equilibrium within 5 h of contact time with a removal of 97%. Adsorption quantity was 469 $mg \cdot g^{-1}$ at 293 K. Adsorption equilibrium data can be predicted by Langmuir model and Koble–Corrigan model, while the kinetic adsorption data followed pseudo-second-order model. The thermodynamic results showed that the adsorption was a spontaneous process with endothermic reaction and entropy increasing. LG-loaded adsorbent can be regenerated using 0.010 $mol \cdot L^{-1}$ of NaOH solution.

*Keywords:* PEI-CNTs; Adsorption; Light green; Regeneration

## 1. Introduction

The wastewater containing dyes not only has obvious chromaticity, but also affects the senses, and the organic matter in water will consume dissolved oxygen and deteriorate the environment [1]. Dyes have great biological toxicity and threaten human health seriously, as there is aromatic structure [2]. Dyes can be discharged into water by the production and application of industries such as textile, coating, plastic, food, paper, leather, rubber, ink, and printing industries. The composition of dye's wastewater is complex, and it is difficult to be biodegraded. There are high chromaticity, high toxicity, and high chemical oxygen demand value. So, dye wastewater is difficult to be disposed of. Therefore, it is urgent to purify the dye before the discharge of dye solution into environment [3,4].

The traditional treatment methods of dye wastewater include chemical oxidation, photocatalytic oxidation, electrochemical method, membrane separation technology, ion-exchange method, adsorption method, and biodegradation [5]. In these methods, the adsorption method is considered to be one of the most attractive methods. The adsorption method has the following advantages: low energy consumption, friendly environment, simple and fast, easy operation, high efficiency, and lack of secondary pollution [6,7]. It is one of the most applied wastewater treatment methods.

In recent decades, carbon nanotubes (CNTs) have attracted the attention of scholars worldwide. CNTs were first discovered by Iijim [8] in 1991. CNTs, including single-walled carbon nanotubes (SWCNTs) and multi-walled

* Corresponding author.

carbon nanotubes (MWCNTs), are cylindrical nanostructures composed essentially of carbon atoms in $sp^2$ hybridization [9]. As one type of carbonaceous material, CNTs have abundant pore structure and large specific surface area, which provide a wide range of adsorption sites [10,11]. Because of their surface functional groups and hydrophobic surfaces, CNTs show strong interactions with both organic compounds and heavy metal ions. However, because CNTs are easily reunited in solutions and are difficult to disperse in different solvents, the application of CNTs in many fields is limited. Therefore, the modification of CNTs to improve their dispersibility and adsorption properties has been widely studied.

Functionalization of CNTs is mainly carried out through chemical methods, including pure chemical methods (chemical oxidation and deposition) and extended chemical processes (i.e., electrochemistry, sol-gel, microemulsion, and hydrothermal method) [12]. Peng et al. [13] studied the removal of lead and copper ions in aqueous solution by CNT/magnetic iron oxide composite. Hadavifar et al. [14] reported the adsorption of Hg(II) from wastewater by amino-functionalized MWCNTs and thiol-functionalized MWCNTs. Adsorption isotherm and kinetic data were fitted by Langmuir and pseudo-second-order models, respectively [14]. Huang and Chen [15] studied the removal of Cr(VI) from the wastewater by magnetic MWCNTs. The pseudo-second-order model best explained the kinetic behavior of the adsorption process. The calculated value of the Gibbs free energy demonstrated a spontaneous and endothermic adsorption process [15].

Polyethyleneimine (PEI) with a large number of primary, secondary, and tertiary amines is easily protonated in aqueous solution and has a greater adsorption capacity for the anionic dye. Because of the water solubility of PEI, it is difficult to be directly used as adsorbent in the adsorption of anionic dye. PEI has been grafted onto the surface of various materials via chemically robust covalent bonds to improve the removal capacity of contaminants [16–18].

In this paper, through the cross-linking effect of epichlorohydrin (ECH), PEI was grafted to MWCNTs, and PEI-CNTs were obtained with large amounts of amino groups. PEI-CNTs can be applied to adsorb acidic anionic dyes or heavy metal ions. The aim of this study was to prepare PEI-CNTs nanocomposite for the removal of light green (LG) dyes (anionic dye) from solution. The effect of pH and salt concentration on the adsorption quantity was performed, and the mechanism of adsorption was presented.

## 2. Materials and methods

### 2.1. Materials

Carboxylated MWCNTs (Macklin, Shanghai, China), PEI (molecular weight 10,000 g $mol^{-1}$, Aladdin, Shanghai, China), absolute ethanol (Fuchen Chemical Reagent, Tianjin, China), and ECH (Kermel, Tianjin, China) were used. LG was purchased from Shanghai LanJi Science and Technology Development Co., Ltd. All of the chemical agents were of analytical grade.

### 2.2. Preparation of PEI-CNTs and LG solution

MWCNTs, NaOH, $H_2O$, ethanol, and ECH were added into a conical bottle. The mixtures were placed in a thermostat oscillator and shaken at 30°C for 6 h, then centrifuged and ethanol was added to wash away the excess ECH solution. Next PEI was added and shaken at a constant temperature (30°C) for 4 h, then centrifuged and washed with distilled water to the neutral. Finally, functional MWCNTs can be obtained at the end of the drying process. Compared with MWCNTs, PEI-CNTs was easily dispersed in solution and separated by centrifugation.

Carboxylated MWCNTs with an inner diameter of 2–5 nm, an outer diameter of less than 8 nm, a length of 10–30 μm, and a specific surface area of 500 $m_2 \cdot g^{-1}$ were used in this experiment. LG formula is $C_{37}H_{34}N_2Na_2O_9S_3$, and its molecular weight is 792.88 $g \cdot mol^{-1}$. Dissolve LG in distilled water to prepare the reserve solution (400 $mg \cdot L^{-1}$). The preparation of all working solutions should be diluted with distilled water to the required concentration.

### 2.3. Characterization of CNTs and PEI-CNTs

Several analytical techniques were used to characterize the synthesized products. The microstructure and morphology of MWCNTs and PEI-CNTs were imaged by transmission electron microscope (TEM, TECNAIG2F20-S-TWIN, USA). The characteristic functional groups were determined by Fourier-transform infrared spectroscopy (FTIR Spectrometer, Nicolet iS50, USA). Raman spectroscopy (Raman, LabRAM HR Evolution, France) was used to determine the structure of MWCNTs and PEI-CNTs. The binding energy of PEI-CNTs before and after the adsorption of LG was analyzed by X-ray photoelectron spectroscopy (XPS, ESCALAB 250Xi, England).

### 2.4. Adsorption experiments

The removal of LG from aqueous solution by PEI-CNTs was studied in batch mode. A certain amount of adsorbent (solid mass/solution volume, 0.80 $g \cdot L^{-1}$) was added to a 50 mL conical flask, and then 10 mL of LG solution was added at an initial concentration of 400 $mg \cdot L^{-1}$. Then the conical flasks were placed in thermostatic shaker (Guohua enterprise SHZ-82, China) at 120 rpm. After adsorption, PEI-CNTs were separated from solution by centrifugation at 5,000 $rpm \cdot min^{-1}$ and LG concentration can be measured. Referring to the standard curve of LG at the maximum wavelength (633 nm), the concentration of LG in the supernatant was measured and calculated by spectrophotometer. (752, Shanghai Shun Yu Hengping Science Instrument Co., Ltd, China).

The effect factors included the following: (1) effect of pH: the pH value of the solution was adjusted in the range of 3–10 by 0.1 $mol \cdot L^{-1}$ NaOH and 0.1 $mol \cdot L^{-1}$ HCl solution, at a constant temperature of 303 K, PEI-CNTs; (2) effect of salt concentration: within the range of 0–0.20 $mol \cdot L^{-1}$ in the solution of NaCl and $Na_2SO_4$ at a constant temperature of 303 K with pH 3, PEI-CNTs; (3) effect of contact time and temperature: the solution concentration is 400 $mg \cdot L^{-1}$ (50–360 min) at temperatures 293, 303, and 313 K with pH 3; and (4) effect of LG concentration with solution: pH 3.0 at temperatures 293, 303, and 313 K, respectively.

The adsorption quantity of LG loaded onto unit weight of PEI-CNTs was calculated using the following equation:

$$q_e = \frac{V(c_0 - c_e)}{m} \quad (1)$$

where $V$ is the LG solution volume (L), $c_0$ is the initial LG concentration (mg·L$^{-1}$), $c_e$ is the LG concentration at any time $t$ or equilibrium (mg·L$^{-1}$), and $m$ is the mass of PEI-CNTs (g).

### 2.5. Desorption study

The LG-loaded PEI-CNTs were obtained for LG adsorption at an initial concentration of 400 mg·L$^{-1}$ (pH 3) and a temperature of 303 K. Then, they were washed with distilled water to remove unadsorbed dye and dried at 333 K. The exhausted adsorbent was regenerated by 0.010 mol·L$^{-1}$ NaOH solution. The regenerated adsorbent was reused at the same experimental conditions. The regeneration yield was obtained as the ratio of values of $q_e$ before and after regeneration.

## 3. Results and discussion

### 3.1. Characterization of MWCNTs and PEI-MWCNTs

#### 3.1.1. TEM analysis

The TEM images of MWCNTs and PEI-CNTs are recorded in Fig. 1. It is observed from Fig. 1(a) that it was well dispersible, there were no impurities on the surface of MWCNTs, and its structure was relatively complete and smooth. The surface of PEI-CNTs became rough and the diameter of the tube became thick, and there was a substance covering the surface from Fig. 1(b), which was a molecular coating of PEI after the graft reaction.

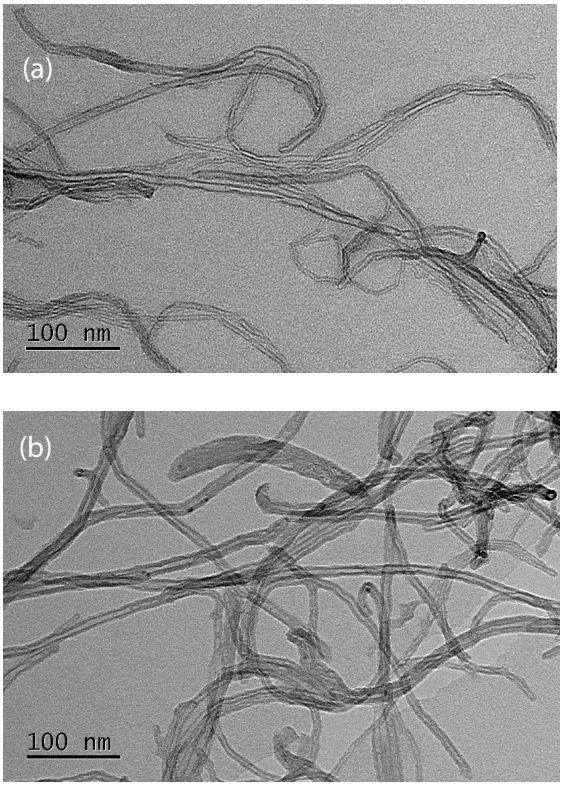


Fig. 1. TEM images of (a) MWCNTs and (b) PEI-CNTs.

#### 3.1.2. FTIR analysis

To confirm the type of functional groups on the CNTs before and after modification, FTIR spectra were performed and shown in Fig. 2. In the wave number 3,400 cm$^{-1}$, there was a relatively wide strong peak, which was the stretching vibration of the –OH and –NH. The strong peak at 2,921 cm$^{-1}$ was the vibration peak of $-CH_3$ and $-CH_2$. The absorption peak at 1,710 cm$^{-1}$ was due to the stretching vibration of C=O [19]. The absorption peak at 1,622 cm$^{-1}$ was the characteristic absorption peak of the C–N vibration. Absorption at 1,000–1,200 cm$^{-1}$ was from vibration of C–O existed in MWCNTs. The main difference between the infrared spectra of PEI-CNTs and MWCNTs in the Fig. 2 was that the peak at 1,710 cm$^{-1}$ from vibration of C=O became very weak and the peak at 3,440 cm$^{-1}$ was enhanced from N–H stretching vibration, which indicated that a large number of amino groups were introduced on the MWCNTs surface. Therefore, it can be concluded that PEI was successfully grafted onto MWCNTs.

#### 3.1.3. Raman analysis

The Raman spectra of CNTs were also generally performed. The Raman characterization results of MWCNTs and PEI-CNTs are shown in Fig. 3. Peak on the left is the D band (disturbance band), which is caused by the lattice defect of the curved layer. The peak of the G band on the right is the scatting peak of tubular graphite structure caused by C=C and C–C [20]. The area ratio of the two absorption peaks ($I_D/I_G$) represents the order degree of the surface of the CNTs (disturbance degree) [21].

It can be seen from Fig. 3 that the position of D and G peaks in the modified MWCNTs shifted from 1,345.12 and 1,581.47 cm$^{-1}$ to 1,349.88 and 1,584.55 cm$^{-1}$. This may be the interaction between PEI and MWCNTs resulting in a shift in the peak position. $I_D/I_G$ of the MWCNTs was 1.09. After the

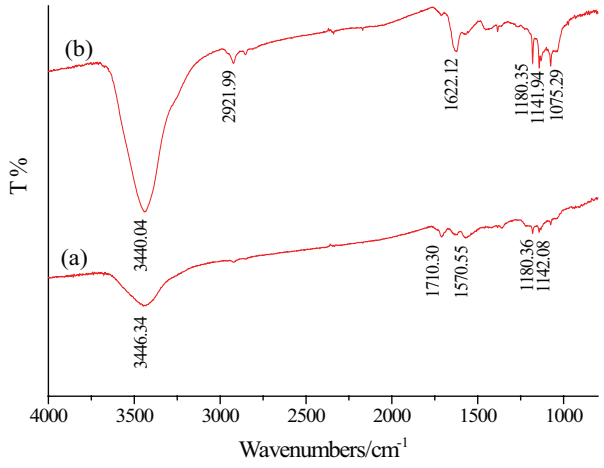


Fig. 2. FTIR spectra of (a) MWCNTs and (b) PEI-CNTs.

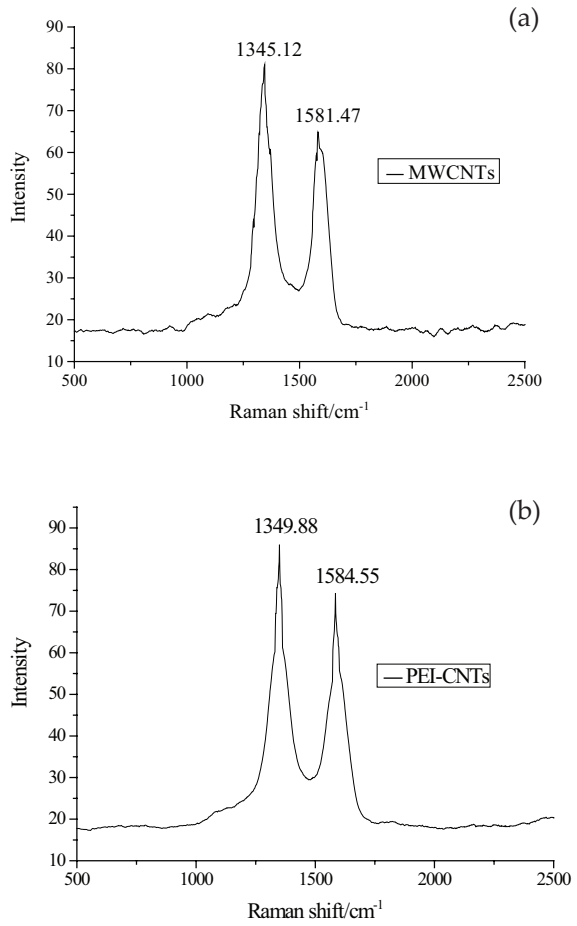


Fig. 3. Raman spectra of (a) MWCNTs and (b) PEI-CNTs.

modification of PEI, $I_D/I_G$ was 1.01. The location of D and G bands of CNTs did not change much before and after modification, and there was no significant difference in the ratio of their area. Thus, it was referred that the basic structure of MWCNTs after PEI modification does not change significantly. As there was no change in symmetric vibration of C=C and C–C existed in CNTs and a very small change in asymmetric vibration of dipole moment, there were no obvious peaks near 1,583 $cm^{-1}$ in FTIR. However, the change of electronic cloud was significant during vibration of C=C and C–C, and there was strong Raman scattering peak at this location.

#### 3.1.4. XPS analysis

The surface chemical composition of raw and chemically modified granule was investigated using XPS (Figs. 4(a) and (b)). It is seen from Fig. 4(a) that PEI-CNTs mainly contained C, O, and N elements, where the N element mainly came from PEI. The element content was 87.58%, 4.77%, and 7.65%, respectively. Broadly speaking, the XPS analysis provided further evidences for the successful preparation of PEI-CNTs. It is seen from Fig. 4(b) that the S2p peak appeared at the binding energy of 168.31eV after adsorption of LG on PEI-CNTs, which indicated that LG could be adsorbed onto the surface of PEI-CNTs.

Figs. 4(c)–(f) show the peak diagram of N1s and O1s before and after adsorption of LG by PEI-CNTs. It was observed that the fitted N1s peak can be assigned to –NH, =N–, $–NH_2$, and $–NH_3^+$ [22–24]. The XPS spectrum of O1s can be deconvoluted into two different peaks at 531.73 and 533.40 eV [25]. After adsorption of LG, N1s were mainly divided into two peaks of 399.88 and 402.27 eV, and the corresponding proportions of $–NH_2$ and $–NH_3^+$ were 37.3% and 62.6% in Fig. 4(d), respectively, which was significantly higher than the proportions of $–NH_2$ (28.6%) and $–NH_3^+$ (58.1%) in Fig. 4(c). The position of $–NH_2$ and $–NH_3^+$ shifted from 399.45 and 400.16 eV to 399.88 and 402.27 eV. Comparing the O1s peaks before and after adsorption, the proportion of –OH increased from 64.1% to 78.3%, while the peaks of –OH and $H_2O$ shifted from 531.73 and 533.40 eV to 531.81 and 533.30 eV. These differences indicated that the electrostatic attraction should occur between amino groups on adsorbent surface and the negative group ($–SO_3^-$) on the dye molecule.

### 3.2. Batch adsorption studies

#### 3.2.1. The effect of pH on adsorption

The pH of the solution affects the charge on the surface of the adsorbent and the chemical structure and stability of the dye surface. The effect of solution pH on LG adsorption is showed in Fig. 5. There was beneficial to the adsorption at solution pH 3. But, the adsorption capacity decreased significantly when the pH value was more than 3, so the pH of the working solution was adjusted to 3 in the following experiments. There was positive charge on the surface of PEI-CNTs when the solution pH was lower. LG was anionic dye with negative charge. The adsorption force was mainly electrostatic attraction at lower solution pH. With the increase of solution pH, the electrostatic force was weakened and the adsorption capacity decreased. The similar results about effect of pH were also observed in the study of Methyl Orange adsorption onto cationic surfactant-modified wheat straw [26] and LG adsorption onto *Salvadora persica* powder [27].

At same conditions (adsorbent dose = 0.80 $g·L^{-1}$, $c_0$ = 400 $mg·L^{-1}$, pH = 3, $t$ = 360 min, and $T$ = 303 K), values of $q_e$ were 487 $mg·g^{-1}$ for PEI-CNTs and 109 $mg·g^{-1}$ for MWCNTs, respectively. This confirmed that adsorption ability was significantly enhanced after PEI modification.

#### 3.2.2. The effect of salt concentration on adsorption

In the actual process of wastewater treatment, the wastewater often contains other co-existing inorganic salt ions, and these inorganic salt ions may have an effect on the adsorption quantity. The effect of ionic strength is complicated, and the presence of salts in solution might screen the electrostatic interaction between opposite charges at the surface of adsorbents and adsorbates, resulting in low uptake during adsorption. Therefore, it is necessary to ascertain the effect of ionic strength on removal of dye from solution. The results are illustrated in Fig. 6. It was seen that the increase in the salt concentration resulted in a decrease of LG adsorption. The main reason was that electrostatic attraction was the main process of adsorption. A large number of $Cl^-$ and $SO_4^{2-}$ in salt solution could bind with functional groups on

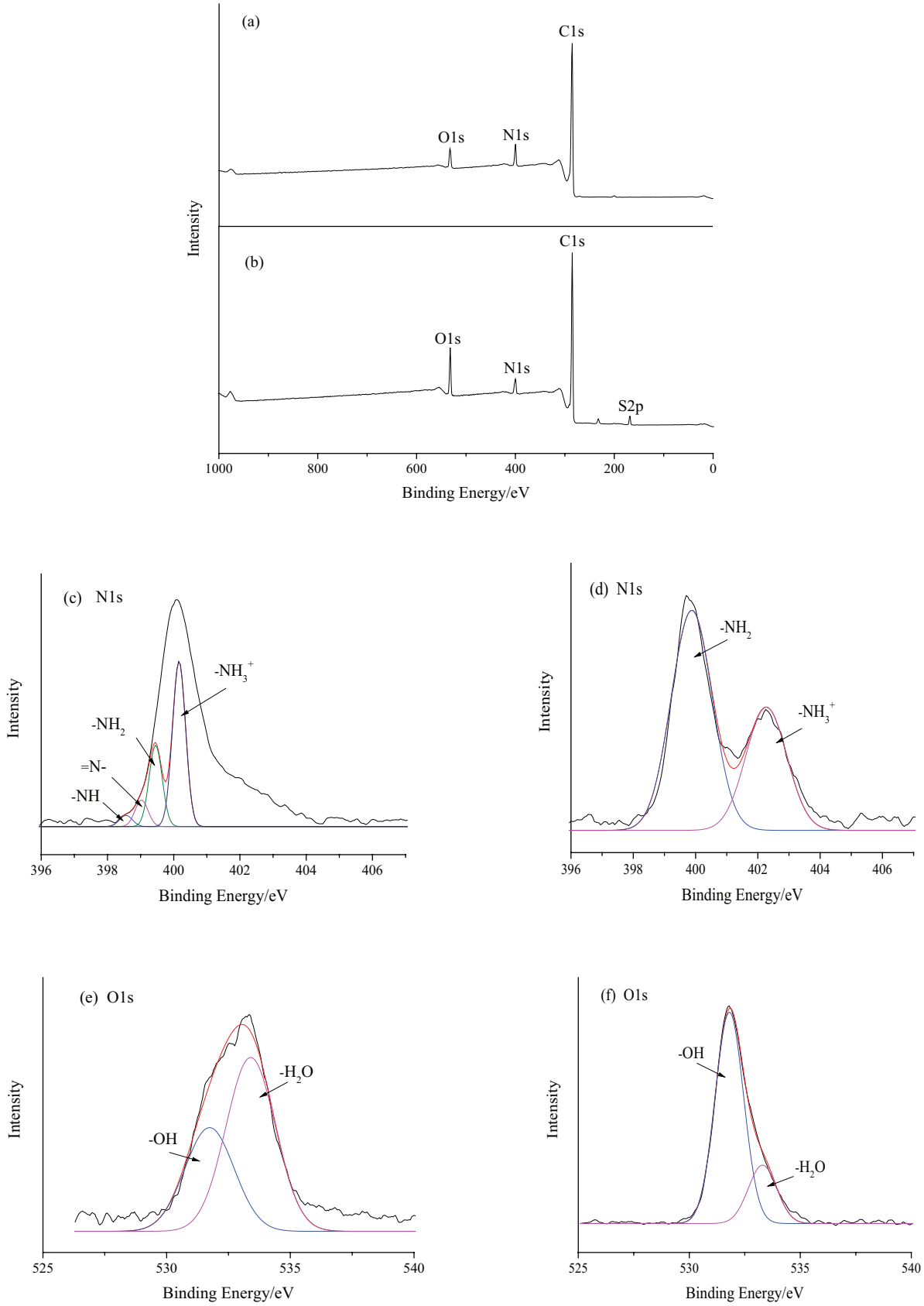


Fig. 4. The survey XPS spectra of (a) PEI-CNTs and (b) PEI-CNTs/LG; high-resolution N1s XPS spectra of (c) PEI-CNTs and (d) PEI-CNTs/LG, and high-resolution O1s XPS spectra of (e) PEI-CNTs and (f) PEI-CNTs/LG.

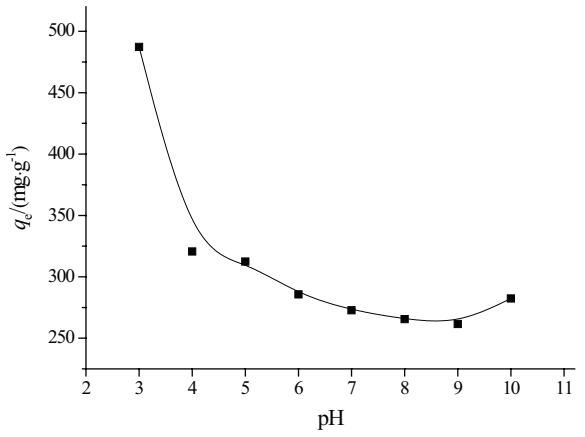


Fig. 5. Effect of solution pH on LG adsorption ($T$ = 303 K, $c_0$ = 400 mg·L$^{-1}$, PEI-CNTs dosage = 0.80 g·L$^{-1}$, and contact time = 300 min).

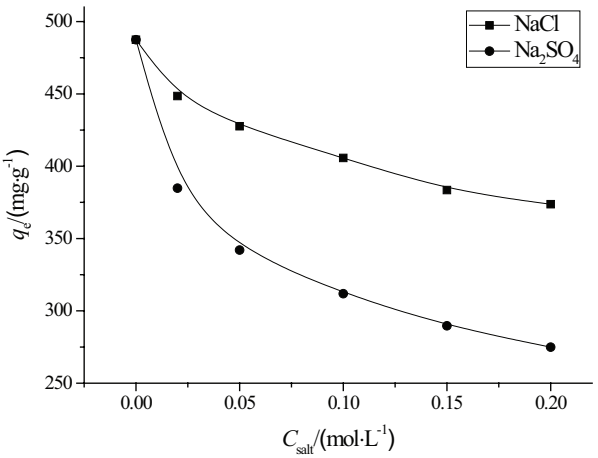


Fig. 6. Effect of NaCl and $Na_2SO_4$ concentration on LG adsorption ($T$ = 303 K, $c_0$ = 400 mg·L$^{-1}$, pH = 3.00, PEI-CNTs dosage = 0.80 g·L$^{-1}$, and contact time = 300 min).

adsorbent surface, which compete with LG for adsorption sites on PEI-CNTs, resulting in the decrease of adsorption capacity [28].

However, even in the salt of 0.20 mol·L$^{-1}$, PEI-CNTs still had a higher adsorption capacity for LG. Therefore, other actions such as hydrogen bond and Van der Waals force were existed during adsorption process. So PEI-CNTs can be used to efficiently remove toxic dyes from textile wastewater. Similar result was observed about LG adsorption onto cationic surfactant-modified wheat straw [29].

### *3.2.3. The effect of contact time on adsorption*

The effect of contact time on LG adsorption onto PEI-CNTs at temperatures 293, 303, and 313 K is illustrated in Fig. 7. It is shown in Fig. 7 that there was a higher adsorption rate for LG adsorption in the initial phase of adsorption (less than 75 min). With the increase of contact time, the adsorption quantity increased and the adsorption tended to dynamic equilibrium at last. Adsorption nearly reached equilibrium at 300 min. According to the results of the experiment, the

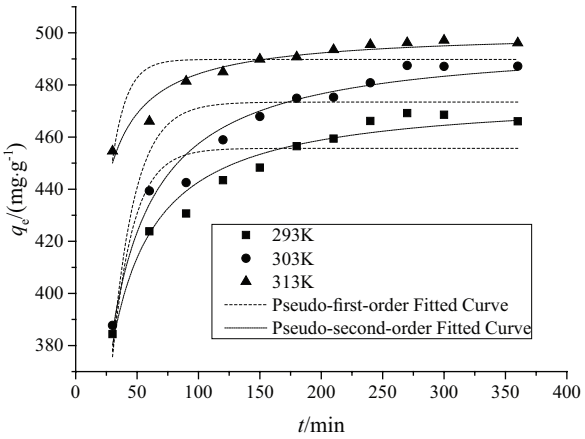


Fig. 7. Effect of contact time on adsorption quantity and kinetic fitted curves ($c_0$ = 400 mg·L$^{-1}$).

agitation time was fixed at 5 h for equilibrium study. It was also seen that there was higher adsorption capacity and faster rate of adsorption at higher temperature.

The study of surface dynamic is related to three parameters: the concentration, time, and temperature of the reaction matter. This paper mainly studied the nonlinear fitting of two kinetic models: pseudo-first-order equation and pseudo-second-order equation. The relative kinetic parameters obtained from two models are given in Table 1.

The pseudo-first-order kinetic model is as follows [30]:

$$q_t = q_e(1 - e^{-k_1 t}) \tag{2}$$

The pseudo-second-order equation can be expressed as follows [30,31]:

$$q_t = \frac{k_2 q_e^2 t}{1 + k_2 q_e t} \tag{3}$$

where $q_t$ and $q_e$ (mg·g$^{-1}$) are the adsorption capacities at time ($t$) and equilibrium, respectively; $k_1$ (min$^{-1}$) and $k_2$ (g·mg$^{-1}$·min$^{-1}$) are the rate constants.

The kinetic data were fitted by nonlinear regressive analysis, and the fitted curves are also shown in Fig. 7. The parameters of kinetic models and determined coefficients ($R^2$) and errors (sum of the squares of the errors [SSE]) are listed in Table 1. From Fig. 7 and Table 1, it is clear that the pseudo-second-order equation is better to fit the experimental data of LG onto PEI-CNTs. The value of $R^2$ was around 0.95, and the error SSE was smaller. This showed that this model could provide a more comprehensive reflection of the adsorption mechanism of LG onto PEI-CNTs when compared with the pseudo-first-order model, and the well-fit pseudo-second-order model implied that the rate-limiting step is chemical adsorption, and the adsorption rate simultaneously depends on the concentration of adsorbents and adsorbates [32,33]. However, the fitting results from the pseudo-first-order equation were relatively poor (with lower values of $R^2$ and higher values of SSE), and this showed that this model was not suitable for describing the kinetic process.

Table 1
Parameters of kinetic models for LG adsorption onto PEI-CNTs

| Pseudo-first-order equation | | | | | |
|---|---|---|---|---|---|
| $T$ (K) | $q_{m(exp)}$ (mg·g$^{-1}$) | $q_{m(theo)}$ (mg·g$^{-1}$) | $k_1 \times 10^{-2}$ | $R^2$ | SSE × 10$^2$ |
| 293 | 469 | 456 ± 4.5 | 5.80 ± 0.58 | 0.721 | 16.7 |
| 303 | 487 | 473 ± 4.8 | 5.34 ± 0.51 | 0.767 | 18.9 |
| 313 | 497 | 489 ± 2.8 | 8.47 ± 0.81 | 0.588 | 7.12 |
| Pseudo-second-order equation | | | | | |
| $T$ (K) | $q_{m(exp)}$ (mg·g$^{-1}$) | $q_{m(theo)}$ (mg·g$^{-1}$) | $k_2 \times 10^{-4}$ | $R^2$ | SSE × 10$^2$ |
| 293 | 469 | 476 ± 2.4 | 2.77 ± 0.21 | 0.965 | 2.10 |
| 303 | 487 | 497 ± 2.6 | 2.30 ± 0.16 | 0.971 | 2.32 |
| 313 | 497 | 500 ± 1.6 | 5.94 ± 0.52 | 0.942 | 1.01 |

Note: SSE = $\Sigma(q-q_c)^2$, where $q$ and $q_c$ are the experimental value and calculated value according to the model, respectively.

*3.2.4. The effect of concentration on adsorption*

The effect of the equilibrium concentration of LG in the solutions on adsorption is shown in Fig. 8. The adsorption quantity increased with the increase of LG equilibrium concentration. This was mainly due to the increase of the concentration gradient on the surface of PEI-CNTs as the concentration of the solution increases, and more adsorbate was bound to the surface of the adsorbent. After the concentration of LG solution reached a certain level, the adsorption site of PEI-CNTs was fully occupied and the adsorption reached saturation, so the adsorption capacity no longer changes. It is also seen from Fig. 8 that the rising temperature was favorable of LG adsorption, indicating that the adsorption process was an endothermic reaction.

Adsorption isotherms can describe how the molecules or ions of adsorbate interact with the surface of adsorbents. Hence, the correlation of equilibrium data using either a theoretical or empirical equation is essential to explain or predict adsorption process. Three common isothermal adsorption equations were used in this paper: Langmuir, Freundlich, and Koble–Corrigan models. The experimental data of LG adsorption onto PEI-CNTs were analyzed by nonlinear fitting. The relative parameters of each model were shown in Table 2.

The Langmuir adsorption isotherm describes monolayer adsorption, which has always been the most widely used adsorption isotherm for solute adsorption in solution [30,34]. The Langmuir isotherm can be expressed as follows:

$$q_e = \frac{q_m K_L c_e}{1 + K_L c_e} \tag{4}$$

where $q_e$ (mg·g$^{-1}$) is the amount adsorbed per unit mass of adsorbent, $q_m$ (mg·g$^{-1}$) is the saturated adsorption amount, $c_e$ (mg·L$^{-1}$) is the equilibrium concentration, and $K_L$ (L·mg$^{-1}$) is a constant that is related to the binding energy.

The Freundlich isotherm expresses adsorption onto a heterogeneous surface [35,36]. The Freundlich isotherm is commonly presented as follows:

$$q_e = K_F c_e^{1/n} \tag{5}$$

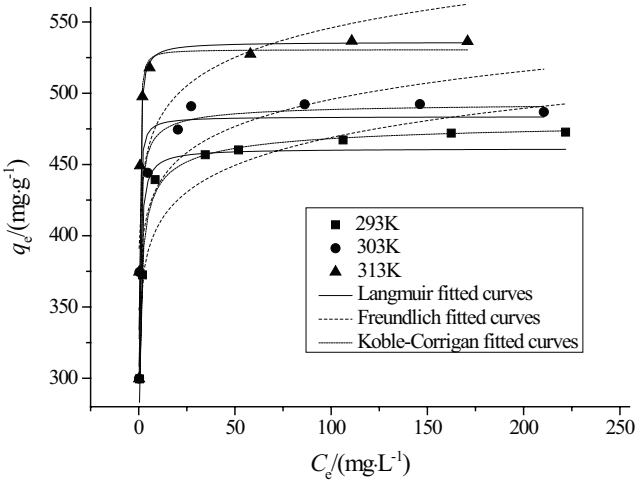


Fig. 8. Adsorption isotherms of LG adsorption onto PEI-CNTs at various temperatures.

where $K_F$ and $n$ are the Freundlich constants characteristic of the system, which are related to the adsorption capacity and adsorption intensity of the sorbent, respectively.

The three-parameter Koble–Corrigan equation is a combination of the Langmuir and Freundlich isotherm-type models [37,38]. It is given by Eq (6).

$$q_e = \frac{AC_e^n}{1 + BC_e^n} \tag{6}$$

where $A$, $B$, and $n$ are the Koble–Corrigan parameters.

The isotherm model parameters were obtained by nonlinear regressive method, and the results are presented in Table 2 while the fitted curves are presented in Fig. 8. From Table 2, the value of $K_L$ was greater than 1 and this indicated the binding force was weak. Compared with values of $R^2$ and SSE listed in table, it was seen that there were higher values of $R^2$ and lower values of SSE from Langmuir model. Furthermore, the fitted curves from Langmuir model were closer to experimental data. So Langmuir model can be used

Table 2
Parameters of adsorption isotherm models for LG adsorption onto PEI-CNTs at different temperatures

| Langmuir | | | | | |
|---|---|---|---|---|---|
| $T$ (K) | $q_{m(\text{theo})}$ (mg·g$^{-1}$) | | $K_L$ | $R^2$ | SSE × 10$^2$ |
| 293 | 461 ± 7.6 | | 3.98 ± 0.67 | 0.912 | 20.3 |
| 303 | 484 ± 5.6 | | 8.46 ± 0.87 | 0.964 | 10.8 |
| 313 | 536 ± 9.1 | | 6.45 ± 0.75 | 0.953 | 21.6 |
| Freundlich | | | | | |
| $T$ (K) | $K_F$ | | 1/$n$ (×10$^{-2}$) | $R^2$ | SSE × 10$^2$ |
| 293 | 353 ± 15 | | 6.15 ± 1.0 | 0.851 | 34.5 |
| 303 | 382 ± 16 | | 5.64 ± 1.1 | 0.813 | 56.6 |
| 313 | 422 ± 23 | | 5.59 ± 1.6 | 0.625 | 172.7 |
| Koble–Corrigan | | | | | |
| $T$ (K) | $A$ | $B$ | $n$ | $R^2$ | SSE × 10$^2$ |
| 293 | 1,241 ± 76 | 2.56 ± 0.19 | 0.524 ± 0.053 | 0.991 | 1.68 |
| 303 | 2,344 ± 485 | 4.74 ± 1.1 | 0.629 ± 0.13 | 0.975 | 6.19 |
| 313 | 4,673 ± 1,767 | 8.81 ± 3.4 | 1.25 ± 0.29 | 0.951 | 18.8 |

to predict the equilibrium process, indicating that the adsorption of LG onto adsorbents can be presumably considered as a monolayer adsorption process.

In the Freundlich isothermal equation, value of $K_F$ increased with the increase of temperature, indicating that the adsorption was an endothermic reaction. The $R^2$ value of the Freundlich model was smaller and the SSE value was higher. Therefore, this model was not suitable for describing the adsorption of LG by PEI-CNTs.

For Koble–Corrigan model, the values of $n$ were close to 1, and this indicated the isotherms were approaching the Langmuir form. The values of $R^2$ were above 0.95 and the values of SSE were lower. The fitted curves from Koble–Corrigan model were closest to the experimental data. These results implied that the Koble–Corrigan model could best be used to describe the adsorption equilibrium behavior.

The values of $q_m$ from Langmuir isotherm of LG adsorption by various adsorbents were compared. At the temperature of 303 K, the adsorption capacity of PEI-CNTs to LG was 487 mg·g$^{-1}$ in this experiment. The adsorption of LG by cationic surfactant-modified peanut husk and wheat straw was 146 and 70.0 mg·g$^{-1}$ [26,29]. As a new biosorbent, *S. persica* (Miswak) powder had an adsorption capacity of 252 mg·g$^{-1}$ for LG [27]. An agricultural industry waste, de-oiled soya, and a waste of thermal power plants, bottom ash, had been tested for their adsorption ability to remove of LG dye from wastewater, and the adsorption capacities were 12.9 and 12.3 mg·g$^{-1}$, respectively [39]. Generally, the adsorption capacity of PEI-CNTs to LG was higher than other adsorbents.

### 3.3. Thermodynamic parameters of adsorption

In order to estimate the effect of temperature on the adsorption of LG onto PEI-CNTs, the free energy change (Δ$G$°), enthalpy change (Δ$H$°), and entropy change (Δ$S$°) were calculated. The apparent equilibrium constant ($K_c'$) of the adsorption is defined as follows [40]:

$$K_c' = c_{\text{ad},e} / c_e \tag{7}$$

where $c_{\text{ad},e}$ (mg·L$^{-1}$) is the concentration of LG on the adsorbent at equilibrium. The value of $k_c$ can be obtained with the lowest experimental LG concentration. The value of $k_c$ was used in the following equation to determine the Gibbs free energy of adsorption (Δ$G$°).

$$\Delta G^0 = -RT \ln K_c' \tag{8}$$

The enthalpy (Δ$H$°) and entropy (Δ$S$°) can be obtained from the slope and intercept of van't Hoff equation of Δ$G$° vs. $T$:

$$\Delta G° = \Delta H° - T\Delta S° \tag{9}$$

where Δ$G$° (J) is standard Gibbs free energy change, $R$ is universal gas constant, 8.314 J·mol$^{-1}$·K$^{-1}$, and $T$ (K) is absolute temperature.

The activation energy ($E_a$) is a physical quantity related to the rate of reaction, and its value can be used to infer the speed of the adsorption process. The activation energy for LG adsorption was calculated by the Arrhenius equation, the linear form is as follows:

$$\ln k_2 = \ln k_0 - E_a / RT \tag{10}$$

where $k_0$ (g·mg$^{-1}$·min$^{-1}$) is the temperature-independent factor, $E_a$ (kJ·mol$^{-1}$) is the apparent activation energy of the reaction of adsorption, $R$ is the gas constant, 8.314 J·mol$^{-1}$·K$^{-1}$, and $T$ (K) is the adsorption absolute temperature. When ln $k_2$ is plotted vs. 1/$T$, a straight line with slope $-E_a/R$ is obtained.

Table 3
Thermodynamic parameters of LG adsorption onto PEI-CNTs

| $E_a$ | $\Delta H°$ | $\Delta S°$ | $\Delta G°$ (KJ·mol$^{-1}$) | | |
|---|---|---|---|---|---|
| (kJ·mol$^{-1}$) | (KJ·mol$^{-1}$) | (J·mol$^{-1}$·K$^{-1}$) | 293K | 303K | 313K |
| 28.6 | 2.70 | 62.3 | −15.6 | −16.1 | −16.8 |

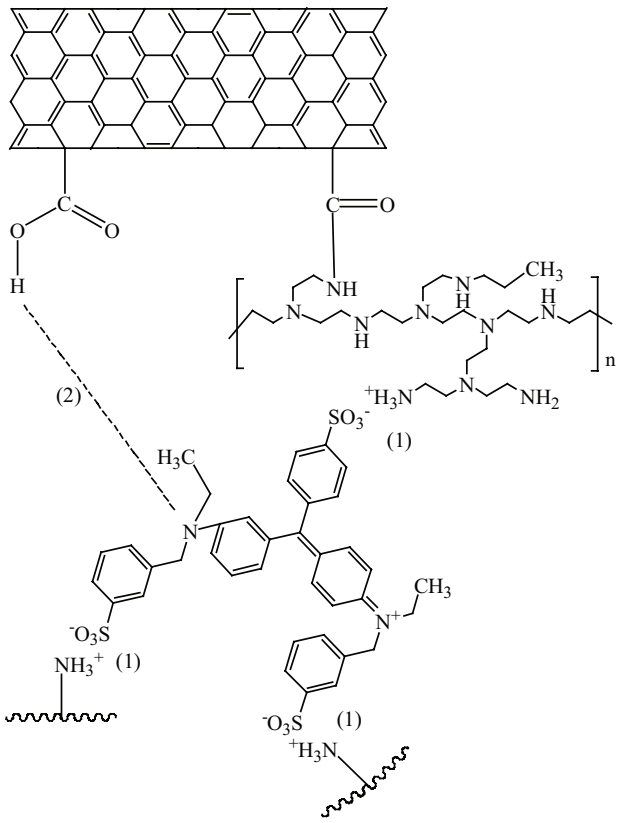


Fig. 9. LG–PEI-CNTs interaction: (1) ionic interaction (involves pH of experimental solution 3) and (2) hydrogen bonding between hydroxyl group of carbon nanotubes and electronegative element in the LG molecule.

Thermodynamic parameters were calculated and listed in Table 3. At the temperature of the experiment, the negative $\Delta G°$ values of LG adsorption onto PEI-CNTs signified the spontaneous nature of the process. In addition, the larger absolute value of $\Delta G°$ at high temperature indicated that the amount of LG adsorption increased with the rise in temperature. The positive value of $\Delta H°$ showed that the reaction was an endothermic reaction, and also showed that the higher temperature was beneficial to the reaction. This may be due to adsorbent swelling, superior dye diffusion rate, and low solution viscosity. The positive $\Delta S°$ values illustrated that the reaction was the process of entropy increase, and it suggested the increased randomness at the solid–solution interface during adsorption of LG on PEI-CNTs, reflecting principally the extra translational entropy gained by the solvent molecules [41]. The value of $E_a$ was 28.6 kJ·mol$^{-1}$, which was less than 40 kJ·mol$^{-1}$, and it was generally believed that there was physical adsorption in the adsorption process.

### 3.4. Desorption and regeneration experiments

Recycle of adsorbent and recovery of adsorbate will make the treatment process economical [42–44]. The regeneration of LG-loaded PEI-CNTs was performed by chemical treatment using 0.010 mol·L$^{-1}$ NaOH as an elution solution. The desorption efficiency was 71.9%, 43.8%, and 31.7%, respectively. The regeneration rate of three cycles was over 80%. It could be considered that NaOH destroys the interaction between adsorbent and LG and releases the occupied active sites. The adsorption capacity of PEI-CNTs for LG was higher than MWCNTs after three desorption and regeneration experiments. In general, PEI-CNTs can be used as practical and renewable adsorbents.

### 3.5. Mechanism of LG adsorption

The functional group of PEI contains a large number of amino groups and can interact with dye molecules. In acidic conditions, the amine –$NH_2$ of the PEI molecule on the surface of the adsorbent was protonated to –$NH_3^+$, the sulfonate group of the reactive dye was dissociated and converted to anionic ions, and the electrostatic interaction between these two counter ions and forms an ion pair. As the pH of the solution increases, the electrostatic attraction between the dye molecules and the adsorbent decreases or the electrostatic repulsion force increases, which result in the decrease of adsorption capacity. Therefore, the predominant adsorption mechanism was electrostatic interactions between the anionic groups of dye and the cationic groups of PEI under acidic conditions [45]. However, there was still a certain adsorption capacity at higher pH values, thus, in addition to ionic bonds, N, S, and O on LG molecules may form hydrogen bond with –COOH groups or –$NH_2$ groups on the surface of adsorbent. Fig. 9 represents the possible interactions between PEI-CNTs and LG.

## 4. Conclusion

PEI-CNTs was successfully prepared and used to adsorb LG from solution in batch mode. The lower pH value of the solution was beneficial to the adsorption, and the existence of salts was negative to adsorption. The Langmuir model and Koble–Corrigan model fitted the equilibrium data well, and the pseudo-second-order kinetic model can better describe the process of LG adsorption, which indicated that the adsorption was single molecular layer and chemical adsorption process. The adsorption was spontaneous and endothermic. The regeneration of LG-loaded PEI-CNTs was effective by NaOH solution and the exhausted PEI-CNTs can be reused. Therefore, it may be concluded that the PEI-CNTs could be an efficient viable alternative for removal of anionic dye from wastewater.

## References

[1] J. Luan, P.-X. Hou, C. Liu, C. Shi, G.-X. Li, H.-M. Cheng, Efficient adsorption of organic dyes on a flexible single-wall carbon nanotube film, J. Mater. Chem. A, 4 (2016) 1191–1194.
[2] Z.H. Huang, Y.Z. Li, W.J. Chen, J.H. Shi, N. Zhang, X.J. Wang, Z. Li, L.Z. Gao, Y.X. Zhang, Modified bentonite adsorption of organic pollutants of dye wastewater, Mater. Chem. Phys., 202 (2017) 266–276.

[3] E. Forgacs, T. Cserhati, G. Oros, Removal of synthetic dyes from wastewaters: a review, Environ. Int., 30 (2004) 953–971.
[4] V.K. Gupta, Suhas, Application of low-cost adsorbents for dye removal—a review, J. Environ. Manage., 90 (2009) 2313–2342.
[5] T.A. Nguyen, R.-S. Juang, Treatment of waters and wastewaters containing sulfur dyes: a review, Chem. Eng. J., 219 (2013) 109–117.
[6] V. Nair, R. Vinu, Peroxide-assisted microwave activation of pyrolysis char for adsorption of dyes from wastewater, Bioresour. Technol., 216 (2016) 511–519.
[7] K. Chinoune, K. Bentaleb, Z. Bouberka, A. Nadim, U. Maschke, Adsorption of reactive dyes from aqueous solution by dirty bentonite, Appl. Clay Sci., 123 (2016) 64–75.
[8] S. Iijim, Helical microtubules of graphitic carbon, Nature, 354 (1991) 56–58.
[9] A. Peigney, Ch. Laurent, E. Flahaut, R.R. Bacsa, A. Rousset, Specific surface area of carbon nanotubes and bundles of carbon nanotubes, Carbon, 39 (2001) 507–514.
[10] V.K. Gupta, R. Kumar, A. Nayak, T.A. Saleh, M.A. Barakat, Adsorptive removal of dyes from aqueous solution onto carbon nanotubes: a review, Adv. Colloid Interface Sci., 193–194 (2013) 24–34.
[11] O.G. Apul, T. Karanfil, Adsorption of synthetic organic contaminants by carbon nanotubes: a critical review, Water Res., 68 (2015) 34–55.
[12] M.M. Khin, A.S. Nair, V.J. Babu, R. Murugan, S. Ramakrishna, A review on nanomaterials for environmental remediation, Energy Environ. Sci., 5 (2012) 8075–8109.
[13] X. Peng, Z. Luan, Z. Di, Z. Zhang, C. Zhu, Carbon nanotubes-iron oxides magnetic composites as adsorbent for removal of Pb(II) and Cu(II) from water, Carbon, 43 (2005) 880–883.
[14] M. Hadavifar, N. Bahramifar, H. Younesi, Q. Li, Adsorption of mercury ions from synthetic and real wastewater aqueous solution by functionalized multi-walled carbon nanotube with both amino and thiolated groups, Chem. Eng. J., 237 (2014) 217–228.
[15] Y. Huang, X. Chen, Carbon nanomaterial-based composites in wastewater purification, Nano Life, 4 (2014) 1441006.
[16] Z. Chen, S. Deng, H. Wei, B. Wang, J. Huang, G. Yu, Polyethylenimine-impregnated resin for high $CO_2$ adsorption: an efficient adsorbent for $CO_2$ capture from simulated flue gas and ambient air, ACS Appl. Mater. Interfaces, 5 (2013) 6937–6945.
[17] Y. Shang, J.H. Zhang, X. Wang, R.D. Zhang, W. Xiao, S.S. Zhang, R.P. Han, Use of polyethylenemine-modified wheat straw for adsorption of Congo red from solution in batch mode, Desal. Wat. Treat., 57 (2016) 8872–8883
[18] L. Shen, L. Zhang, M. Chen, X. Chen, J. Wang, The production of pH-sensitive photoluminescent carbon nanoparticles by the carbonization of polyethylenimine and their use for bioimaging, Carbon, 55 (2013) 343–349.
[19] E. Murugan, S. Arumugam, New dendrimer functionalized multi-walled carbon nanotube hybrids for bone tissue engineering, RSC Adv., 4 (2014) 35428–35441.
[20] A.C. Ferrari, J. Robertson, Interpretation of Raman spectra of disordered and amorphous carbon, Phys. Rev. B: Condens. Matter, 61 (2000) 14095–14107.
[21] L.R. Hou, L. Lian, D.K. Li, G. Pang, J.F. Li, X.G. Zhang, S.L. Xiong, C.Z. Yuan, Mesoporous N-containing carbon nanosheets towards high-performance electrochemical capacitors, Carbon, 64 (2013) 141–149.
[22] C. Ling, F.-Q. Liu, C. Long, T.-P. Chen, Q.-Y. Wu, A.-M. Li, Synergic removal and sequential recovery of acid black 1 and copper (II) with hyper-crosslinked resin and inside mechanisms, Chem. Eng. J., 236 (2014) 323–331.
[23] S.B. Hartono, S.Z. Qiao, K. Jack, B.P. Ladewig, Z. Hao, M. Lu, Improving adsorbent properties of cage-like ordered amine functionalized mesoporous silica with very large pores for bioadsorption, Langmuir, 25 (2009) 6413–6424.
[24] T.P. Chen, F.Q. Liu, C. Ling, J. Gao, C. Xu, L.J. Li, A.M. Li, Insight into highly efficient coremoval of copper and p-nitrophenol by a newly synthesized polyamine chelating resin from aqueous media: competition and enhancement effect upon site recognition, Environ. Sci. Technol., 47 (2013) 13652–13660.
[25] D.J. Kang, X.L. Yu, S.R. Tong, M.F. Ge, J.C. Zuo, C.Y. Cao, W.G. Song, Performance and mechanism of Mg/Fe layered double hydroxides for fluoride and arsenate removal from aqueous solution, Chem. Eng. J., 228 (2013) 731–740.
[26] Y.Y. Su, Y.B. Jiao, C.C. Dou, R.P. Han, Biosorption of methyl orange from aqueous solutions using cationic surfactant-modified wheat straw in batch mode, Desal. Wat. Treat., 52 (2014) 6145–6155.
[27] E.A. Moawed, A.B. Abulkibash, Selective separation of Light green and Safranin O from aqueous solution using *Salvadora persica* (Miswak) powder as a new biosorbent, J. Saudi Chem. Soc., 20 (2016) S178–S185.
[28] J. Shen, G. Huang, C.J. An, S. Zhao, S. Rosendahl, Immobilization of tetrabromobisphenol A by pinecone-derived biochars at solid-liquid interface: synchrotron-assisted analysis and role of inorganic fertilizer ions, Chem. Eng. J., 321 (2017) 346–357.
[29] Y.Y. Su, B.L. Zhao, W. Xiao, R.P. Han, Adsorption behavior of light green anionic dye using cationic surfactant-modified wheat straw in batch and column mode, Environ. Sci. Pollut. Res., 20 (2013) 5558–5568.
[30] Y. Liu, Y.-J. Liu, Biosorption isotherms, kinetics and thermodynamics, Sep. Purif. Technol., 61 (2008) 229–242.
[31] R.P. Han, L.J. Zhang, C. Song, M.M. Zhang, H.M. Zhu, L.J. Zhang, Characterization of modified wheat straw, kinetic and equilibrium study about copper ion and methylene blue adsorption in batch mode, Carbohydr. Polym., 79 (2010) 1140–1149.
[32] J. Shen, G. Huang, C.J. An, X.Y. Xin, C. Huang, S. Rosendahl, Removal of Tetrabromobisphenol A by adsorption on pinecone-derived activated charcoals: synchrotron FTIR, kinetics and surface functionality analyses, Bioresour. Technol., 247 (2018) 812–820.
[33] J.Y. Yang, X.Y. Jiang, F.P. Jiao, J.G. Yu, The oxygen-rich pentaerythritol modified multi-walled carbon nanotube as an efficient adsorbent for aqueous removal of alizarin yellow R and alizarin red S, Appl. Surf. Sci., 436 (2018) 198–206.
[34] R.P. Han, J.J. Zhang, P. Han, Y. Wang, Z.H. Zhao, M.S. Tang, Study of equilibrium, kinetic and thermodynamic parameters about methylene blue adsorption onto natural zeolite, Chem. Eng. J., 145 (2009) 496–504.
[35] M.Y. Han, Q.G. Wang, H. Li, L.Y. Fang, R.P. Han, Removal of methyl orange from aqueous solutions by polydopamine mediated surface functionalization of $Fe_3O_4$ in batch mode, Desal. Wat. Treat., 115 (2018) 271–280.
[36] R.D. Zhang, J.H. Zhang, X.N. Zhang, C.C. Dou, R.P. Han, Adsorption of Congo red from aqueous solutions using cationic surfactant modified wheat straw in batch mode: kinetic and equilibrium study, J. Taiwan Inst. Chem. Eng., 45 (2014) 2578–2583.
[37] Z.L. Wu, H. Yang, F.-P. Jiao, Q. Liu, X.-Q. Chen, J.-G. Yu, Carbon nanoparticles pillared multi-walled carbon nanotubes for adsorption of 1-naphthol: thermodynamics, kinetics and isotherms, Colloids Surf., A, 470 (2015) 149–160.
[38] J.Y. Song, W.H. Zou, Y.Y. Bian, F.Y. Su, R.P. Han, Adsorption characteristics of methylene blue by peanut husk in batch and column mode, Desalination, 265 (2011) 119–125.
[39] A. Mittal, J. Mittal, A. Malviya, D. Kaur, V.K. Gupta, Decoloration treatment of a hazardous triarylmethane dye, Light Green SF (Yellowish) by waste material adsorbents, J. Colloid Interface Sci., 342 (2010) 518–527.
[40] Z. Aksu, Determination of the equilibrium, kinetic and thermodynamic parameters of the batch biosorption of nickel(II) ions onto *Chlorella vulgaris*, Process Biochem., 38 (2002) 89–99.
[41] S.S. Tahir, N. Rauf, Removal of a cationic dye from aqueous solutions by adsorption onto bentonite clay, Chemosphere, 63 (2006) 1842–1848.
[42] R.P. Han, Y. Wang, Q. Sun, L.L. Wang, J.Y. Song, X.T. He, C.C. Dou, Malachite green adsorption onto natural zeolite and reuse by microwave irradiation, J. Hazard. Mater., 175 (2010) 1056–1061.

[43] J.S. Liu, W.X. Liu, Y.R. Wang, M.J. Xu, B. Wang, A novel reusable nanocomposite adsorbent, xanthated $Fe_3O_4$-chitosan grafted onto graphene oxide, for removing Cu(II) from aqueous solutions, Appl. Surf. Sci., 367 (2016) 327–334.
[44] Y.C. Rong, H. Li, L.H. Xiao, Q. Wang, Y.Y. Hu, S.S. Zhang, R.P. Han, Adsorption of malachite green dye from solution by magnetic activated carbon in batch mode, Desal. Wat. Treat., 106 (2018) 273–284.
[45] D.H.K. Reddy, S.-M. Lee, Application of magnetic chitosan composites for the removal of toxic metal and dyes from aqueous solutions, Adv. Colloid Interface Sci., 201–202 (2013) 68–93.